Quantum Features of PXRC Angular Distributions From Relativistic Channeled Electrons in a Crystal

K B Korotchenko, Yu L Pivovarov

Department of Theoretical and Experimental Physics, National Research Tomsk Polytechnic University, 30, Lenin Avenue, Tomsk, 634050, Russia

E-mail: `korotchenko@tpu.ru`

Abstract. We predict quantum features in angular distributions of parametric X-radiation from channeled relativistic electrons (PXRC). The effect is connected with the number of quantum states of channeled electrons, form-factors of the transverse quantum channeling states and initial populations of these quantum states. The main motivation of this work is theoretical prediction for the future experiment at the SAGA-LS facility.

1. Introduction
Recent experiments [1, 2, 3] on studies of angular distributions of parametric X-radiation from 255 MeV channeled electrons (PXRC) in a Si crystal showed some differences between of that distribution and standard angular distribution of parametric X-radiation (PXR) from non-channeled electron. According [1], this difference is connected with manifestation of two quantum effects: a) form-factors of the transverse quantum states of channeled electrons; b) initial populations of these quantum states. The band structure of transverse quantum states in a periodic planar channeling potential sufficiently influences the form-factors and initial populations of these states. As a result, the angular distribution of PXRC changes with appearance of every new quantum channeling state following increase of the electron beam energy.

2. Basic equations
According [1], the formula for angular distribution of PXRC intensity from planar channeled electrons captured into a transverse quantum state with a number n reads:

$$I_{\text{PXRC}}^n = \frac{d^3 N_{nn}}{d\theta_x d\theta_y dz} = I_{\text{PXR}} \left| F_{nn}(q) \right|^2, \tag{1}$$

here $q = (\boldsymbol{\kappa} - \mathbf{g})_y = \omega_B \theta_y / c$ and I_{PXR} is the standard angular distribution of PXR intensity near the Bragg direction calculated in a two-wave approximation:

$$I_{\text{PXR}} = \frac{\alpha \omega_B}{16\pi c \sin^2 \theta_B} \left[\frac{\theta_x^2}{1 + W_\pi^2} + \frac{\theta_y^2}{1 + W_\sigma^2} \right], \tag{2}$$

θ_x, θ_y – the angular coordinates counted from the Bragg direction $\boldsymbol{\kappa}_B$ and θ_B – the Bragg angle defined by [4] $\sin \theta_B = |\mathbf{v}_\parallel \mathbf{g}| / (\text{v}_\parallel g)$ – see, in figure 1, $\hbar \omega_B = 2\pi \hbar c / d$ – energy of PXRC photon

(we consider the first allowed order of the Bragg reflection), d – spacing between the channeling planes, $\boldsymbol{\kappa}$ – the wave vector of PXRC photon and $\mathbf{g}$ – reciprocal lattice vector (see, in figure 1).

Figure 1. The angular coordinates θ_x and θ_y, describing angular distribution of PXRC near the Bragg direction $\boldsymbol{\kappa}_B$, and mutual arrangement of the vector of longitudinal velocity $\mathbf{v}_\parallel$, wave vector $\boldsymbol{\kappa}$ of PXRC photon and $\mathbf{g}$ – reciprocal lattice vector: (a) 3D view; (b) the schematics of mutual arrangement of the vectors.

The important quantity entering Eq.(1) is the form-factor of the transverse quantum channeling state with the number n:

$$F_{nn}(q) = \int_{-d/2}^{d/2} \varphi_n^*(y) exp(-\mathrm{i}qy)\varphi_n(y)dy, \tag{3}$$

Here, $\varphi_n(y)$ is the wave function of channeled electron in a quantum state with the number n. Other quantities entering Eq.(2) are [5, 6]:

$$
\begin{aligned}
W_\tau &= \frac{1}{2\,|\chi_g|\,\Gamma_\tau}\left(R - \frac{|\chi_g|^2\Gamma_\tau^2}{R}\right), \\
R &= \theta_x^2 + \theta_y^2 + \theta_{kin}^2, \; \theta_{kin}^2 = \gamma^{-2} + |\chi_0|, \\
\Gamma_\pi &= \cos 2\theta_B, \; \Gamma_\sigma = 1, \; \tau = (\pi, \sigma),
\end{aligned}
\tag{4}
$$

here $\gamma = E/mc^2$ is the relativistic factor of electron, χ_0, χ_g – the Fourier components of the local electric susceptibility of a crystal.

The angular distribution of PXRC from electrons planar channeled in a crystal is calculated using the following formula [1, 2, 3]:

$$
\begin{aligned}
I_{\mathrm{PXRC}} &= \sum_n^N I_{\mathrm{PXRC}}^n P_n(\theta_0) \\
&= I_{\mathrm{PXR}} \sum_n^N P_n(\theta_0)|F_{nn}(q)|^2,
\end{aligned}
\tag{5}
$$

where N is number of bound channeling states and

$$P_n(\theta_0) = \frac{1}{d}\left|\int_{-d/2}^{d/2} e^{\mathrm{i}p\theta_0 y/\hbar}\varphi_n(y)dy\right|^2, \tag{6}$$

is the the initial population [7] of the n-th quantum state depending on the angle of incidence θ_0 of electron beam with respect to the channeling planes (p is initial momentum of electrons). Looking at Eqs.(3, 5, 6) one may conclude that the angular distribution of PXRC depends on the number of quantum channeling states, on the wave functions of these states and on the angle of incidence θ_0.

Let us further consider the simplest case of PXRC, when the angle of incidence $\theta_0 = 0$. In this case, only sub-barrier (bound channeling states) are populated. As is known [7], the number of those channeling states increases proportionally $\sqrt{\gamma}$. When the beam energy increases, the new quantum channeling states appear and contribute to the sum in Eq.(5), every with its own form-factor F_{nn} and population $P_n(\theta_0)$. Therefore, an appearance of every new quantum channeling state will lead to a change in the PXRC intensity.

3. Beyond the separate plane approximation

The "true" wave functions for (220) planar channeling in Si crystal used in further numerical calculations have been obtained using the method described in [6, 8].
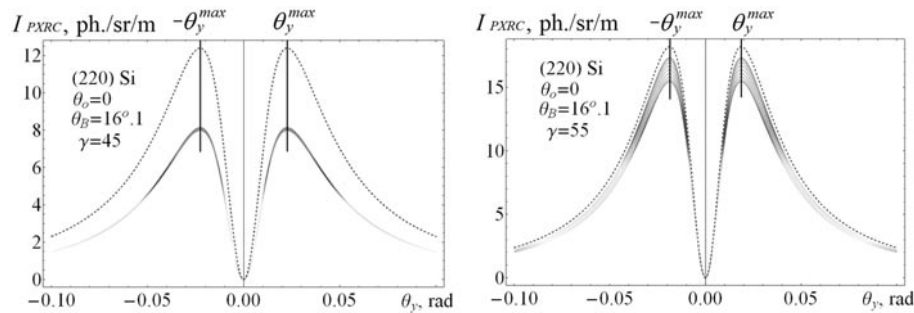

Figure 2. PXRC and PXR (dashed line) angular distribution calculated with the "true" periodic planar (220) Si channeling potential: a) for $\gamma = 45$ and the number of bound channeling states $N = 4$; b) for $\gamma = 55$ and $N = 5$. The increase of the number of bound states N manifests itself as $\sim 200\%$ increase in I_{PXRC} intensity. The maximums of I_{PXRC} are located at $\theta_y = \pm\theta_y^{max}$. In fact, the PXRC intensity graphs are not single lines but rather broad bands. We illustrated this drawing 10 lines (inside the band) corresponding to 10 positions inside transverse energy band of planar channeled electrons. In figure 2a the width of the band is small and these 10 lines are invisible, while in figure 2b the lines are visible and form the broad band.

In figure 2 we presented PXRC angular distributions calculated with the periodic planar (220) Si channeling potential for two values of relativistic factor in a vicinity of the "quantum jump": $\gamma = 45$ corresponds to the number of bound channeling states $N = 4$ and $\gamma = 55$ corresponds to $N = 5$.

To each line on the graph of PXRC in figure 2 corresponds a certain part of energy band of the channeled electron transverse motion. For calculation the each band was divided into 10 equal parts (by the transverse momentum) as it described in [6, 8]. As the result, the PXRC intensity graphs are not single lines but rather broad bands. We illustrated this drawing 10 lines (inside the band) corresponding to 10 positions inside transverse energy band of planar channeled electrons.

The difference in magnitudes of I_{PXRC} in figure 2 is explained by the influence of the band structure of energies and corresponding "true" wave functions on the transverse form-factors and initial populations.

At the same time the PXRC intensity increases by almost a factor of two, following increase of γ from 45 up to 55. The reason is that into Eq.(1), besides form-factors $|F_{nn}|^2$, enter initial

populations $P_n(\theta_0)$.

In figure 3 we present PXRC angular distributions calculated with the periodic planar (220) Si channeling potential for two values of relativistic factor: $\gamma = 460$ corresponds to the number of bound channeling states $N = 14$ and $\gamma = 480$ corresponds to $N = 15$.
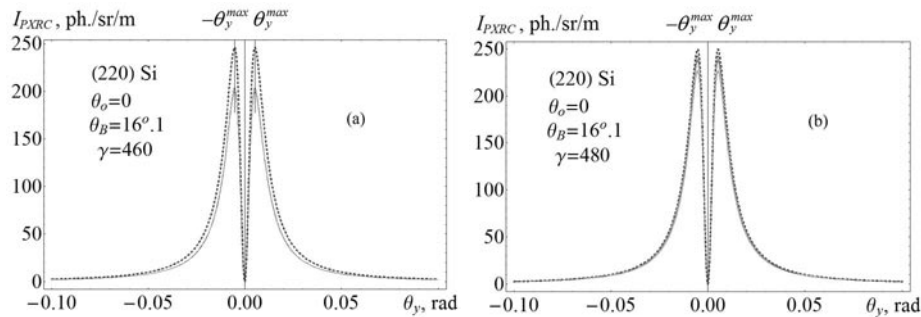

Figure 3. PXRC and PXR (dashed line) angular distribution calculated with the "true" periodic planar (220) Si channeling potential: a) for $\gamma = 460$ the number of bound channeling states $N = 14$; b) for $\gamma = 480 \Longrightarrow N = 15$. Here, the increase of the number of bound states N manifests itself as $\sim 20\%$ increase in I_{PXRC} intensity. The maximums of I_{PXRC} are located at $\theta_y = \pm\theta_y^{max}$. As in figure 2, the PXRC intensity graphs are not single lines but rather broad bands.

The electron relativistic factor in the figure 2a and 3 was taken equal to $\gamma = 45, 55$ and $\gamma = 460, 480$, corresponding to the program of planned experiments on PXRC studies with $20 - 255$ MeV electrons at the SAGA-LS accelerator center [1, 2, 3].
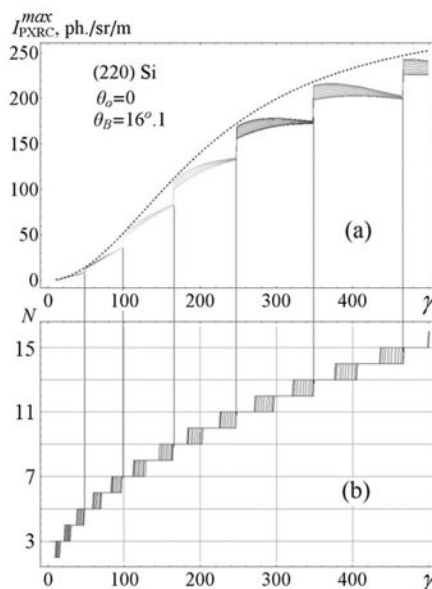

Figure 4. a) The maximums of PXRC and PXR (dashed line) as the function of γ in the (220) Si (along the plane $\theta_x = 0$). b) The number N of bound channeled states as the function of γ. As in figure 2 and figure 3, the graphs are not single lines but rather broad bands. We illustrated this drawing 10 lines (inside the band) corresponding to 10 positions inside transverse energy band of planar channeled electrons.

The maximums of angular distributions $I_{PXRC}^{max}(\gamma) = I_{PXRC}(\gamma)|_{\theta_y=\theta_y^{max}}$ (in the plane $\theta_x = 0$) as the functions of beam energy are presented in figure 4. The correlation of the number of quantum bound states $N = N(\gamma)$ and values of the maximums of $I_{PXRC}^{max}(\gamma)$ manifests itself at definite γ values. Here, for comparison, we plotted also the maximums of PXR angular distribution (see, in details the Section 4).

4. Comparison of PXRC and PXR

To characterize the difference in angular distributions of PXR and PXRC, we introduce the quantity

$$
\begin{aligned}
\delta &= \delta(\theta_y^{max}; \gamma) = \frac{I_{PXR}^{max} - I_{PXRC}^{max}}{I_{PXR}^{max}} \equiv \\
&\equiv 1 - \sum_n P_n(\theta_0) \left| F_{nn}(\theta_y^{max}) \right|^2,
\end{aligned}
\tag{7}
$$

which depends on the number of quantum states N (a function of relativistic factor γ), initial population of every n-th state (a function of angle of incidence θ_0 and wave function $\varphi_n(y)$). Both $\varphi_n(y)$ and form-factor $F_{nn}(q)$ depend on the relativistic factor.
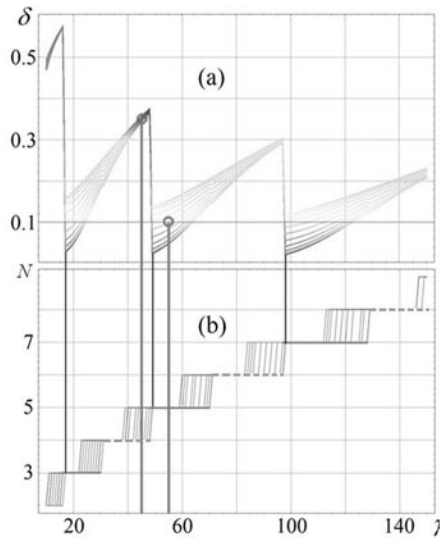

Figure 5. Dependences on relativistic factor γ of: a) maximum values of the $\delta = \delta(\theta_y^{max}; \gamma)$ (formula (7)); b) number N of bound channeling states for (220) planar channeling in a "real" 1D periodic potential Si crystal. Here, the wave functions are obtained numerically following procedure described in [6, 8] and are used to calculate the initial populations $P_n(\theta_0)$ and transverse form-factors $|F_{nn}(\theta_y; \gamma)|^2$. The vertical lines correspond to the values of the relativistic factor $\gamma = 45$ and $\gamma = 55$ (see, figure 2) and the circles at the ends of these lines mark the values of δ, corresponding $I_{PXRC}^{max}(\gamma) = I_{PXRC}(\gamma)|_{\theta_y=\theta_y^{max}}$ in figure 2. The origin of 10 lines is explained in caption to figure 2.

As is well known in quantum mechanics, at least one bound state always exists in a 1D potential well of finite depth. We would like to stress, that in the problem of planar electron channeling there is an additional parameter - relativistic factor of the beam γ, which allows the change of the number N of quantum channeling states.

The evolution of the quantity δ (formula (7)) with the beam energy increasing is presented in figure 5, where we plotted both the number of quantum states $N = N(\gamma)$ and the values

$\delta = \delta(\theta_y^{max}; \gamma)$ taken at the maximums of angular distributions I_{PXR}^{max} and I_{PXRC}^{max} (along the plane $\theta_x = 0$). As one can see, the correlation of the number of quantum bound states $N = N(\gamma)$ and $\delta = \delta(\theta_y^{max}; \gamma)$ manifests itself at the definite γ values.

In figure 3 – figure 5, to each line on the graph corresponds a certain part of energy band of the channeled electron transverse motion (as in figure 2).

In figure 5, the band structure of transverse quantum channeling states (sequence of periodicity of planar channeling potential) decreases the value of transverse form-factor squared $|F_{nn}|^2$ and, in addition, sufficiently changes the values of initial populations $P_n(\theta_0)$ of quantum states. Both two factors increase the difference in angular distributions of PXRC and PXR, i.e. increase the δ value.

5. Conclusions

To summarize, as it was first suggested in [1], the difference in angular distributions of the standard Parametric X-Radiation (PXR) from plane-wave electrons (no channeling) and Parametric X-Radiation from channeled electrons (PXRC) is connected with manifestation of two quantum effects: form-factors of transverse quantum channeling states and their initial populations. In the present work we showed that this difference has non-trivial dependence on the electron beam energy: it undergoes some quantum jumps with appearance of the new quantum channeling states following increase of the electron beam energy. The magnitude of the jump depends on form-factors and initial populations of these quantum states.

The experimental studies of predicted quantum features in PXRC angular distributions are planned with 20 .. 255 MeV electrons at the accelerator center SAGA-LS [1, 2, 3].

6. Aknowledgements

References

[1] Korotchenko K B, Pivovarov Yu L and Takabayashi Y 2012 JETP Lett. **95** 8 433
[2] Korotchenko K B, Pivovarov Yu L and Takabayashi Y 2013 Nucl. Instrum. Methods Phys. Res. **B**309 25
[3] Takabayashi Y, Korotchenko K B, Pivovarov Yu L and Tukhfatullin T A 2013 Nucl. Instrum. Methods Phys. Res. **B**315 105
[4] Baryshevsky V G, Feranchuk I D and Ulyanenkov A P 2005 *Parametric X-ray Radiation in Crystals* (Berlin: Springer)
[5] Yabuki R, Nitta H, Ikeda T and Ohtsuki Y H 2001 Phys. Rev. B **63** 174112
[6] Bogdanov O V, Korotchenko K B and Pivovarov Yu L 2007 JETP Lett. **85** 11 555
[7] Bazylev V A, Zhevago N K 1987 *Radiation of Fast Particles in Matter and External Fields* [in Russian] (Moscow: Nauka)
[8] Bogdanov O V, Fiks E I, Korotchenko K B and Pivovarov Yu L 2010 Journal of Physics: Conference Series 1 236